

Computer Simulation for Transient Flow in Oil-free Scroll Compressor

Genfu Xiao^{1,2} and Guoping Liu¹

¹*School of Mechanical and Electrical Engineering, Nanchang University, Nanchang, China*

²*School of Mechanical and Electrical Engineering, Jinggangshan University, Ji'an, China*

xiaogenfu@163.com

Abstract

In this paper, the numerical simulation of the two-dimensional and three-dimensional transient flow field in an oil-free scroll compressor is performed by the CFD dynamic mesh technique. During the procedure of simulation, the air in the scroll compressor is treated as ideal gas, and fit for the flow governing equations as well as gas state equation. In our approach, RNG $k-\epsilon$ model is used for turbulent model. The simulation results show that the flow field in the scroll compressor is time-periodic, in addition, the generation, motion and size change of the vortices inside the scroll compressor can be visualized. By contrasting the two-dimensional and three-dimensional flow field, the advantages and disadvantages are clearly found in simulation. The simulation not only extremely vividly reveals the scroll compressor inherent laws but also provides theoretical references for the optimal design of scroll compressors.

Keywords: *Scroll Compressor, Dynamic Mesh, Flow Field, 2D Simulation, 3D Simulation*

1. Introduction

Compared with piston compressors, scroll compressors currently have obviously competitive advantages in the air conditioning field with its high efficiency and low noise. The flow and heat transfer processes of scroll compressors are very complex, and a lot of scholars have done multitude studies over the past years. The thermodynamic process was analyzed and the mathematical models of scroll compressors were established[1-3]. Nevertheless, it's difficult to meet the general laws of scroll compressor flow field by these simplified models. With the rapid development of computer technology, computational fluid dynamics is used to study the flow field of compressors, which can get detailed flow field information and reveal potential physical process.

In the field of positive displacement compressors, many achievements have been achieved by using CFD technology. YueXiangji et al applied dynamic mesh technique in the analysis of rotary compressors transient flow and displayed visualized flow field in compression chamber[4]. Ma Yitai et al utilized dynamic mesh technique to simulate the transient flow field in rolling rotor expander[5-6]. Kovacevic et al studied the screw compressor compression chamber mesh generation technology in detail, using CFD software to calculate the three-dimensional flow parameters in screw compressor compression chambers[7-9].

CFD rarely applied in the field of scroll compressors and the researchers are few in number. Most of conclusions have not been fully validated. N.stosic simulated simply internal flow field of screw compressors and scroll compressors[10].S.Pietrowicz et al made a two-

dimensional scroll compression chamber simulation using commercial mathematical software[11], Ooi simulated the internal flow field of a scroll compressor, and analyzed thermal conductivity in the scroll compressor[12].

In this dissertation, reasonable physical and mathematical models of oil-free scroll compressor are established. Dynamic mesh technique is applied in two-dimensional and three-dimensional transient flow field numerical simulation. The method of dynamic mesh is described in detail. The flow field is shown in the case of different crank angle. At last, the results of 2D and 3D flow field are contrasted and the simulation is verified by experiment.

2. Theoretical Models

2.1. Physical Models

Scroll compressors are the gas compression machinery by means of the volume change. After assembly of fixed scroll and orbiting scroll, a number of closed crescent-shaped volumes can be formed. As shown in Figure 1.

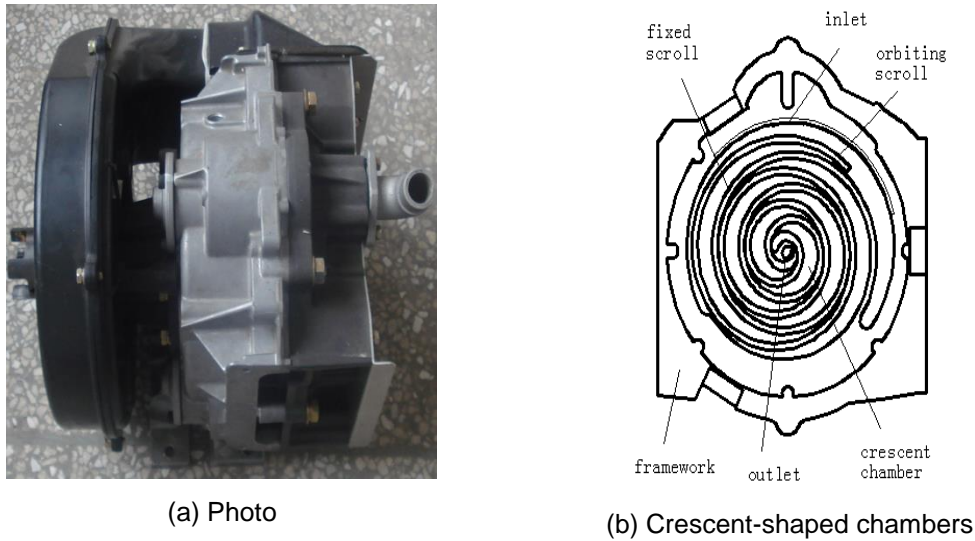


Figure 1. Scroll Compressor

When the eccentric shaft promotes the orbiting scroll to round the fixed scroll center, the volume of compression chambers expands or shrinks. Thereby the suction, compression and exhaust of gas are realized.

2.2. Control Equations

The summation of the time-averaged flow and the instantaneous pulsating flow may express turbulent flow, namely time average method:

$$u = \bar{u} + u', v = \bar{v} + v', w = \bar{w} + w', p = \bar{p} + p' \quad (1)$$

The fluid control equation using formula (1) can be expressed as follows:

$$\frac{\partial \bar{u}}{\partial t} + \text{div}(\bar{u}\bar{u}) = -\frac{1}{\rho} \frac{\partial \bar{p}}{\partial z} + \mu \text{div}(\text{grad} \bar{u}) + \left[\frac{\partial \bar{u}'^2}{\partial x} - \frac{\partial \bar{u}'v'}{\partial y} - \frac{\partial \bar{u}'w'}{\partial z} \right] \quad (2)$$

$$\frac{\partial \bar{v}}{\partial t} + \text{div}(\bar{v}\bar{u}) = -\frac{1}{\rho} \frac{\partial \bar{p}}{\partial y} + \mu \text{div}(\text{grad} \bar{v}) + \left[-\frac{\partial \bar{u}'v'}{\partial x} - \frac{\partial \bar{v}'^2}{\partial y} - \frac{\partial \bar{v}'w'}{\partial z} \right] \quad (4)$$

$$\frac{\partial \bar{w}}{\partial t} + \text{div}(\bar{w}\bar{u}) = -\frac{1}{\rho} \frac{\partial \bar{p}}{\partial z} + \mu \text{div}(\text{grad} \bar{w}) + \left[-\frac{\partial \bar{u}'w'}{\partial x} - \frac{\partial \bar{v}'w'}{\partial y} - \frac{\partial \bar{w}'^2}{\partial z} \right] \quad (5)$$

Formula (2) is mass conservation equation and formula (3)~(5) are momentum conservation equations. Where, \bar{u} is time-averaged velocity vector. \bar{u} , \bar{v} and \bar{w} are x, y, z direction component of \bar{u} , respectively. u' , v' , w' is x, y, z direction component of fluctuating velocity vector, respectively. μ is dynamic viscosity and ρ is the density of ideal-gas. \bar{p} is the mean pressure and p' is fluctuating pressure.

Because there is internal swirling flow in scroll compression chambers during the rotation of the orbiting scroll, RNG k - ε turbulence model is selected. Equation k and equation ε can be expressed respectively as follows:

$$\frac{\partial(\rho k)}{\partial t} + \frac{\partial(\rho k u_i)}{\partial x_i} = \frac{\partial}{\partial x_j} \left[\alpha_k \mu_{eff} \frac{\partial k}{\partial x_j} \right] + G_k + \rho \varepsilon \quad (6)$$

$$\frac{\partial(\rho \varepsilon)}{\partial t} + \frac{\partial(\rho \varepsilon u_i)}{\partial x_i} = \frac{\partial}{\partial x_j} \left[\alpha_\varepsilon \mu_{eff} \frac{\partial \varepsilon}{\partial x_j} \right] + \frac{C_{1\varepsilon}^* \varepsilon}{k} G_k + C_{2\varepsilon} \rho \frac{\varepsilon^2}{k} \quad (7)$$

Where, k is turbulent kinetic energy. ε is kinetic energy dissipation rate. μ_t is turbulent viscosity. μ_{eff} is the correction value to turbulent viscosity in RNG k - ε turbulence model.

In low Reynolds number flow region near the wall, wall function method is capable of solving the flow problems of the near-wall region, which can be expressed by the following equation:

$$\mu^+ = \frac{1}{k} \ln(E y^+), \quad y^+ = \frac{\Delta y_p C_\mu^{1/4} k_p^{1/2}}{\mu} \quad (8)$$

Where, y^+ and μ^+ are the dimensionless parameters which denote the distance and the velocity. Δy_p is the distance between the node and wall. k_p is the turbulent kinetic energy of the node p and E is the constant about wall roughness.

The formulae mentioned above are suitable to calculate 3D flow field. If coordinate z is removed from those formulae, they are suitable to calculate 2D flow field, too.

2.3. Dynamic Mesh Models

The dynamic mesh technique may simulate the transient flow field whose geometry changes over time. The temporal change of the flow field in compressors can be captured by utilizing this technique. The dynamic mesh is realized through ALE coordinates in this article.

The dynamic mesh quality equation, momentum equation and energy equation under ALE coordinates are showed as follows. The volume force, and the heat source such as radiation and chemical reaction have not considered in the equations.

$$\frac{\partial}{\partial t} \iiint_V \rho d\sigma + \iint_S \rho(V - x_c) \cdot n ds = 0 \quad (9)$$

$$\frac{\partial}{\partial t} \iiint_V \rho V d\sigma + \iint_S [\rho(V - x_c) \cdot n] V ds = \iint_S [P]_n ds \quad (10)$$

$$\frac{\partial}{\partial t} \iiint_v \rho \left(\frac{|V|^2}{2} + e \right) d\sigma + \iint_s [\rho(V - x_c) \cdot n] \left(\frac{|V|^2}{2} + e \right) ds = \iint_s [P]_n \cdot V ds + \iint_s \lambda \nabla T \cdot n ds \quad (11)$$

Where, $[P]_n$ is the component of the stress tensor in the surface, including static pressure and viscous force.

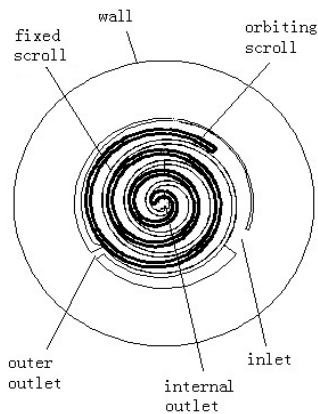
3. Solution Method

3.1. Geometry Simplification

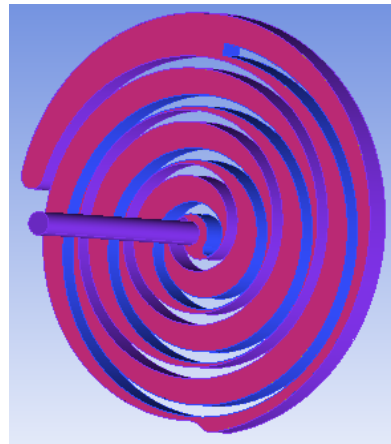
The configuration of real compressor shown in figure 1(a) is very complex, so the geometric model must be simplified.

A two-dimensional compressor model is established in CAD software shown in figure 2(a). Scroll compressor is put in a circular container. The outermost circle indicates container wall and there is ideal gas between the scroll compressor and the container wall. The intake port is provided in the side wall of the scroll compressor. Ideal gases enter the compressor from this port.

The arrangement of exhaust port is very difficult. The real exhaust port perpendicular to the plane is difficult to achieve in a two-dimensional simulation. The exhaust port is opened on the stationary scroll as shown in figure 2(a). The internal outlet and outer outlet are related by hollow scroll wall.



(a) 2D model



(b) 3D model

Figure 2. Geometric Models

Scroll compressor is composed of compression chamber and exhaust pipe in 3D simulation. The exhaust pipe can't be found in 2D simulation. The exhaust hole is opened in the side of the scroll compressor as a real scroll compressor. The scroll wall height is lower than the real compressor's in order to decrease the computer time.

3.2. Meshing

For two-dimensional scroll compressor, unstructured triangular mesh is divided in the whole calculation domain. The yellow domain is triangular mesh shown in figure 3. The scroll compressor and the surrounding air are divided into two computational

domains. Different size grid is applied to these two calculation domain in order to decrease the computer time.

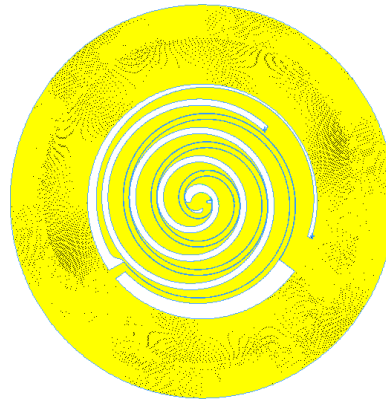
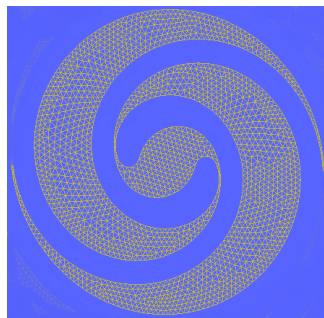
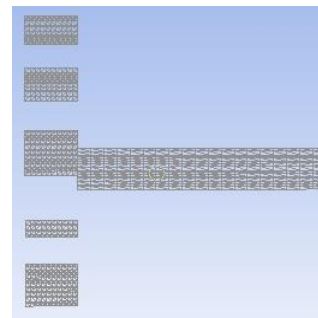


Figure 3. Meshes in 2D Simulation

For three-dimensional scroll compressor, the computational domain is the fluid domain in scroll compressor. The shape of compressor and exhaust pipe is simplified in order to facilitate calculation. Meshing is completed in commercial software as shown in figure 4. There are about 280000 grid cells. The computational domains consist of the compressor domain and exhaust pipe domain. The computational domain of the compressor is made up of prism grid cell. The computational domain of the exhaust pipe is composed of hexahedral grid cell. Two computational domains are related by interface which ensures the correction of calculation when orbiting scroll reach exhaust port.



(a) Lateral view



(b) Front view

Figure 4. Meshes in 3D Simulation

As shown in figure 4, triangular mesh can be found in front view, which may change to prismatic grid after longitudinal tensile. The prismatic grid guarantees that the dynamic method of spring smoothing and local remeshing can apply correctly.

3.3. Parameter Setting

Dynamic method is needed because the shape of compression chambers changes following the change of crank angle. Only dynamic mesh in all existing CFD technique can achieve this dynamic simulation. In dynamic mesh method, when the orbiting scroll

moves slightly, the edges of the meshes are seen as a spring, deforming slightly with orbiting scroll. When the orbiting scroll moves fast and meshes deformation exceeds a certain limit, meshes need dividing again.

The orbiting scroll movement is not a pure rotation, but the rigid body movement around an axis. The orbiting scroll enable to receive the move law through the macro DEFINE_CG_MOTION provided by FLUENT. The macro in UDF is set as follow:

```
DEFINE_CG_MOTION( )  
{ cg_vel[0] = R*sin(time*2πf) *2πf;  
  cg_vel[1] = - R*cos(time*2πf) *2πf; }
```

DEFINE_CG_MOTION is the macro controlling the movement of edges. cg_vel[0] is x-direction line speed. cg_vel[1] is y-direction line speed. Time is current simulation time. R is the radius of rotation. F is the frequency of rotation.

For three-dimensional simulation, the z-coordinate remains invariant when meshes move. When the x-coordinate and y-coordinate of grid changes, the dynamic mesh method combined spring smoothing and local remeshing are utilized for the purpose of improving the quality of grid after deformation.

The finite volume method is employed in the whole process. The PRESTO! method is adopted to calculate pressure term and the PISO algorithm is utilized to solve the pressure-velocity coupling equation.

4. Simulation Results and Analysis

4.1. Convergence Process

Residuals are the sum of flux through every face in cell. The sum of flux through every face should be equal to zero theoretically. For the reason of numerical accuracy, it is not possible to gain zero residuals. In other words, the residuals should be as small as possible.

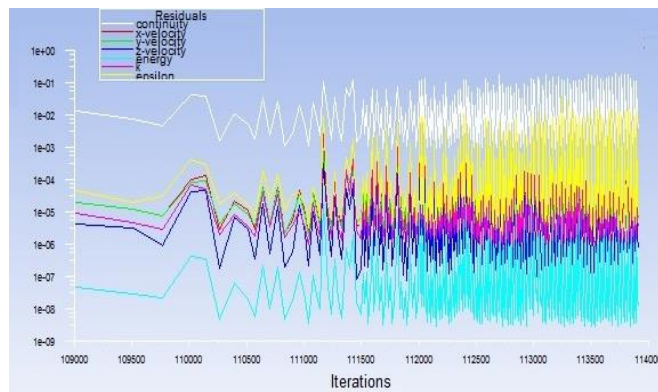


Figure 5. Convergence Process

In this paper the convergence condition is residuals less than 10^{-3} . Because the energy items can converge easily, its residuals are set less than 10^{-6} . As shown in figure 5, it seems that residual curves can't converge due to the repetitive oscillation. Actually, it's capable of convergence in every step. The oscillation is the result of continuous iteration which is caused by meshes movement.

4.2. CFD Results of 2D Simulation

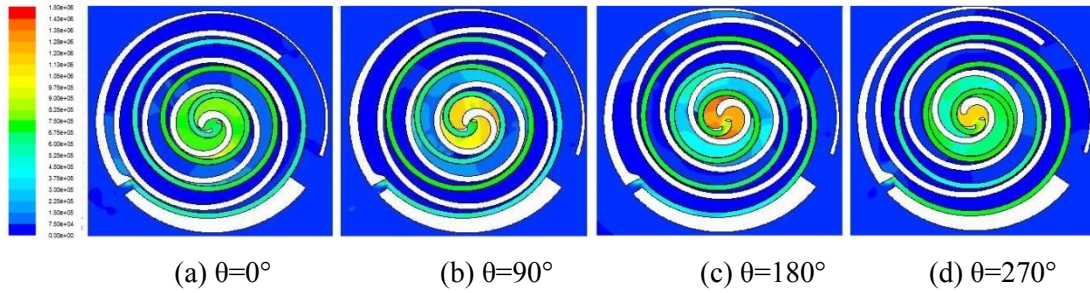


Figure 6. Distribution of Pressure in 2D Simulation

The pressure in compression chambers during suction, compression, exhaust are shown as Figure 6. With narrowing of compression chambers, gas pressure increases gradually. Maximum average pressure appeared in the center compression chamber, which meets the theoretical laws of pressure change. The maximum pressure appears in the place of scrolls engagement for the greatest speed change.

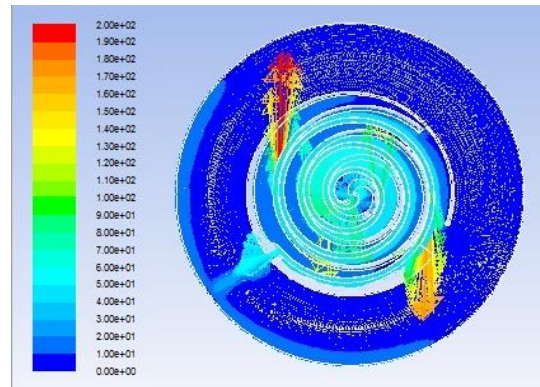


Figure 7. Speed Field in 2D Simulation

Figure 7 demonstrates the velocity field of the scroll compressor. The maximum velocity appears in the position of scrolls engagement. The air flows from the chambers near the center to the chambers faraway the center.

4.3. 3D CFD Results

3D CFD results can be obtained as follows.

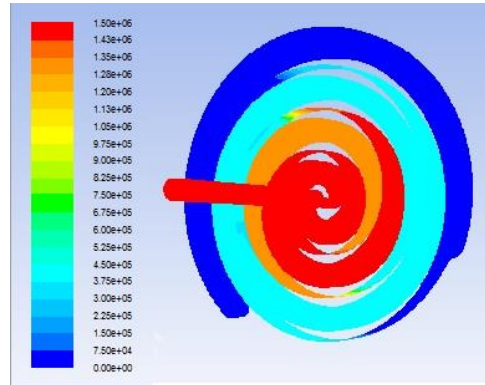
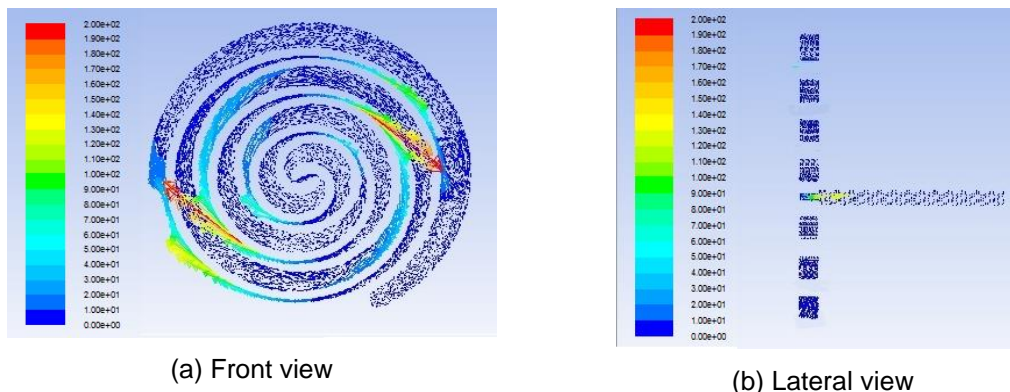


Figure 8. Distribution of Pressure in 3D Simulation

Distribution of pressure in 3D simulation is displayed in figure 8. The pressure in exhaust pipe is the same as the pressure inside the center compression chamber. The pressure in center compression chamber is the largest in all compression chambers, which is the same as 2D simulation.



(a) Front view

(b) Lateral view

Figure 9. Speed Field in 3D Simulation

Figure 9(a) demonstrates the velocity field of the scroll compressor in 3D simulation. The maximum velocity occurs in the position of scrolls engagement. Figure 9(b) displays the flow process in exhaust port. As the volume decreases in the center of the compression chamber, the gas flows from center chamber to exhaust pipe. The area of exhaust port changes with the movement of orbiting scroll. As a result, the flow loss is affected significantly by the movement.

They conform to the thermodynamics theory and fluid dynamics theory. Those indicate that the simulation results are reasonable.

There are some differences between the 2D and 3D simulation. The pressure is more uniform in the 3D simulation than in the 2D simulation. The velocity field disturbances in the center compression chamber are smaller in the 3D simulation than in the 2D simulation. Lateral outlet is the main effect reason of speed field uneven distribution in 2D centre compression chamber. In summary, the 3D simulation possesses stronger consistency in comparison with the 2D results.

4.4. Experimental Verification



Figure 10. Experimental Equipment

We may verify the result through experiment. Due to equipment limitations, the equipment in figure 10 is used to test our scroll compressors. The average displacement of oil-free scroll compressor in the case of different speeds is measured.

The curves shown in figure 11 are the mass flow rate over time in 2D and 3D simulation. After a short start-up process, the gas mass flow rate changes with time period, namely flow becomes a relatively stable process. The center compression chamber becomes gradually smaller and displacement gradually raises as the orbiting scroll angle increases, until the gas in center of the compression chamber discharges completely. Subsequently, the flow drops rapidly and next compression period starts. The simulation value is very close to actual value. The result of 2D simulation is more accurate than 3D simulation. It's closer to the actual value. Interface in 3D simulation is the main reason of accuracy decreasing.

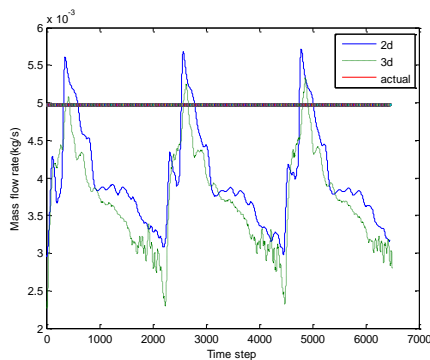


Figure 11. Displacement at Different Time

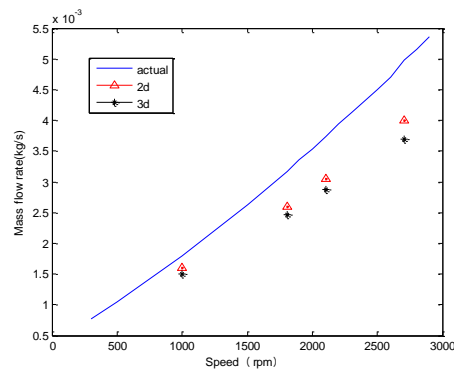


Figure 12. Displacement at Different Speed

The relationship between the mass flow and the measured value in the case of different speeds is shown in figure 12. We may note that the results of 2D simulation are more accurate than the results of 3D. As the speed increases, simulation accuracy declines. In the high-speed case, the larger numerical errors lead to the decline of calculation accuracy.

5. Conclusion

The two-dimensional and three-dimensional flow field simulation models of scroll compressors are established reasonably. The problem how orbiting scroll can move in CFD is solved. The simple and reasonable boundary conditions are identified. The simulation of flow field is realized by using RNG $k-\epsilon$ turbulence models.

By contrasting the 2D and 3D flow field, we may find 2D as well as 3D flow field has its own advantages. The distribution of 3D flow field is more uniform than 2D flow field. It is more consistent with thermodynamic theory. The mass flow rate of 2D flow field is good agreement with the measured values. The vent opening method is the main reason for this difference.

Experimental results show that the results of the flow field simulation are authentic. In addition to the values which are calculated, the simulation results include some intuitive flow field information. Vortex generation, movement, rupture process can be observed obviously. The simulation results can be taken as important references for the further design optimization of oil-free scroll compressors.

References

- [1] Y. Chen, N. P. Halmand E. A. Groll, "Mathematical modeling of scroll compressor-Part I: Compression process modeling", *Int J Refrigeration*, vol.25, (2002), pp.731-750.
- [2] Y. Chen, Halm and P. Nils, "A Mathematical Modeling of Scroll Compressors-Part II: Overall Scroll Compressor Modeling", *International Journal of Refrigeration*, vol.25, (2002), pp.751-764.
- [3] W. Baolong, L. Xianting and S. Wenxing, "A General Geometrical Model of Scroll Compressors Based on Discretional Initial Angles of Involute", *International Journal of Refrigeration*, vol.28, (2005), pp.958-966.
- [4] Y. Xiangji, B. Dechun, S. Zhengyu and Z. Yu, "Moving Mesh Bashed Transient Simulation of Rolling Piston Compressor Pump Chamber Flow", *Journal of Northeastern University(Natural Science)*, vol.32, no.4, (2011), pp.563-566.
- [5] G. Wenjin, M. Yitai and Z. Li, "Simulation and Analysis on CO₂ Rolling Piston Expander", *Journal of Engineering Thermophysics*, vol.31, no.8, (2010), pp.1265-1269.
- [6] M. Yitai, Z. Meilan and T. Hua, "Fluent Simulation and Analysis of CO₂ Two-Cylinder Rolling Piston Expander", *Journal of Tianjin University*, vol.44, no.12, (2011), pp.1093-1099.
- [7] A. Kovacevic, N. Stosic and I. K. Smith, "Numerical Simulation of Fluid Flow and Solid Structure in Screw Compressors", *Proceedings of 2002 ASME Congress, New Orleans*, (2002), pp.1-8.
- [8] A. Kovacevic, "Boundary adaptation in grid generation for CFD analysis of screw compressors", *Int. J. Numer. Meth. Engng.* vol.64, (2005), pp.401-426.
- [9] A. Kovacevic, N. Stosic and I. K. Smith, "The CFD Analysis of A Screw Compressor Suction Flow", *Proceedings of International Compressor Engineering Conference at Purdue, Purdue, USA*, (2000), pp.125-133.
- [10] N. Stosic, I. K. Smith and S. Zagorac, "CFD Studies of Flow in Screw and Scroll Compressor". *Proceedings of International Compressor Engineering Conference at Purdue, Purdue, USA*, (1996), pp.181-186.
- [11] S. Pietrowicz, T. Yanagisawa and M. Fukuta, "Mathematical Modeling of Physical Process in the Scroll Compressor Chamber", *Proceedings of International Compressor Engineering Conference at Purdue, Purdue, USA*, (2002), pp.183-188.
- [12] O. K. Tiow and Z. Jiang, "Convective Heat Transfer in a Scroll Compressor Chamber: A 2-D Simulation", *International Journal of Thermal Sciences*, vol.43, no.7, (2004), pp.677-688.

Authors



Genfu Xiao was born in Ganzhou, China on May 10, 1980 and received the Master's degree in engineering from Nanchang University in 2005. From 2005 he was researcher at Jinggangshan University in school of mechanical and electrical engineering. Since 2009 he is postgraduate at Nanchang University in school of mechanical and electrical engineering. His research interests are related to the simulation and design of scroll compressors. He has authored more than 20 papers published in conference proceedings or journals.



Guoping Liu was born in Linchuan, China on August 1, 1964 and received the PH.D degree in engineering from Zhejiang University in 1999. From 1999 he was teacher at Nanchang University in school of mechanical and electrical engineering. He obtained title of professor in 2006. His research interests include sensing, information processing, modeling and simulation, intelligent control technology. He has authored more than 30 papers published in conference proceedings or journals.

